

6-1-1995

# Computer Simulation Study of the Permeability of Driven Polymers Through Porous Media

Grace M. Foo

*University of Southern Mississippi*

Ras B. Pandey

*University of Southern Mississippi*, [ras.pandey@usm.edu](mailto:ras.pandey@usm.edu)

Follow this and additional works at: [http://aquila.usm.edu/fac\\_pubs](http://aquila.usm.edu/fac_pubs)

 Part of the [Physics Commons](#)

---

## Recommended Citation

Foo, G. M., Pandey, R. B. (1995). Computer Simulation Study of the Permeability of Driven Polymers Through Porous Media. *Physical Review E*, 51(6), 5738-5744.

Available at: [http://aquila.usm.edu/fac\\_pubs/5869](http://aquila.usm.edu/fac_pubs/5869)

This Article is brought to you for free and open access by The Aquila Digital Community. It has been accepted for inclusion in Faculty Publications by an authorized administrator of The Aquila Digital Community. For more information, please contact [Joshua.Cromwell@usm.edu](mailto:Joshua.Cromwell@usm.edu).

## Computer simulation study of the permeability of driven polymers through porous media

Grace M. Foo<sup>1</sup> and R. B. Pandey<sup>1,2</sup>

<sup>1</sup>*The Program in Scientific Computing, University of Southern Mississippi, Hattiesburg, Mississippi 39406-5046*

<sup>2</sup>*Department of Physics and Astronomy, University of Southern Mississippi, Hattiesburg, Mississippi 39406-5046*

(Received 9 January 1995; revised manuscript received 9 March 1995)

A computer simulation model is used to study the permeability of polymer chains driven by a biased flow field through a porous medium in two dimensions. The chains are modeled by constrained self-avoiding walks, which reptate through the heterogeneous medium with a biased probability imposed by the driven field. A linear response description is used to evaluate an effective permeability. The permeability  $\sigma$  shows an unusual decay behavior on reducing the porosity  $p_s$ . We find that the permeability decreases on increasing the bias above a characteristic value  $B_c$ . This characteristic bias shows a logarithmic decay on reducing the porosity,  $B_c \sim -\gamma \ln(1-p_s)$ , with  $\gamma \simeq 0.35$ . The permeability decays with the length ( $L_c$ ) of the chains; at low polymer concentration it shows a power-law decay,  $\sigma \sim L_c^{-\alpha}$ , the exponent  $\alpha$  is nonuniversal and depends on both the porosity as well as the biased field ( $\alpha \simeq 1.64-3.73$ ). We find that the biased field  $B$  and porosity  $p_s$  affect the conformation of the chains. The radius of gyration  $R_g$  of the chains increases with increasing biased field in high porosity, while it decreases on decreasing the porosity at high field bias. In high porosity and low polymer concentrations, the radius of gyration shows a power-law dependence on the chain length,  $R_g \sim L_c^\nu$ , with  $\nu$  depending on the biased field ( $\nu \simeq 0.84-0.94$ ). In order to explain the deviations from the Darcy Law for the polymer flow, a plausible nonlinear response theory via a power-law response formula is suggested; we point out the associated complexities involved in addressing the flow problems in driven polymers.

PACS number(s): 47.55.Mh, 05.60.+w, 82.45.+z, 83.10.Nn

### I. INTRODUCTION

Studying the permeability of porous media [1,2] has attracted considerable interest from ion and mass transport in complex polymer mixtures and molecular permeation in gels (electrophoresis) [3] at small scales to fluid flow through the porous sediments in marine geosciences [4,5] with varied applications such as oil exploration, sedimentation processes, spreading of hazardous waste on the sea floor, etc., at large scale. It is now well known that the shape and size distribution of the pores determine the physical and chemical properties such as permeability and viscoelastic nature of the host porous media. Studying the transport properties of porous media by analytical methods has been severely limited due to their intractabilities in solving the transport equations in highly ramified structures. Computer simulations, on the other hand, are useful in taking into account some of the structural nonlinearities, though they are limited to idealized model systems.

Several attempts [1-10] have recently been made to study the transport properties of interacting particles by lattice gas approaches such as cellular automata, Boltzmann, interacting lattice gas, and hybrid methods. These particulate methods deal with the pointlike particles to study the fluid flow through a porous medium or the conductivity of a heterogeneous material. We know that the transport properties of a heterogeneous media not only depend on the type of the host media (i.e., degree of ramification and porosity) but also on the specific details such as shape, size, mass, etc., of the mobile constituents. Particularly in polymer mixtures, the shape

and size of the molecular species become very important in studying their transport properties [11,12]. To our knowledge, there is no computer-simulation study that has addressed the dependence of permeability on the size and shape of the mobile particles. In this paper we present a computer-simulation model to study the permeability of the constrained self-avoiding chains driven by a biased field through a porous medium. The model is described in the next section which is followed by results and discussion.

### II. MODEL

We consider a two dimensional discrete lattice of size  $L \times L$ . We model the polymer chain of size  $L_c$  by a constrained self-avoiding walk which is generated on the trail of a nonintersecting nonreversible random walk of  $L_c$  steps; this creates a polymer chain of  $L_c + 1$  nodes connected by  $L_c$  links. A site cannot be occupied by more than one node. The polymer-fluid concentration  $p$  is defined as a fraction of sites occupied by the polymer chains. Thus in order to generate a fluid concentration  $p$  of polymer chains on a square lattice of  $N = L^2$  sites we distribute  $N_c$  chains randomly on the lattice where  $N_c = p \times N / (L_c + 1)$ .

Monodisperse barrier particles are distributed randomly in the empty lattice sites with no more than one particle per lattice site. These barrier particles remain immobile throughout the simulation. The empty sites along with the polymer chains, i.e., the sites which are not occupied by the barriers constitute the pores. Thus the random distribution of immobile barrier particles generates a

rigid porous media in which the size of the pores depends on the concentration (i.e., the volume fraction)  $p_b$  of the barriers. The volume fraction of the pore space  $p_s = 1 - p_b$  (i.e., the porosity) is defined as the ratio of the number of pore sites to the total number of lattice sites. The larger the  $p_s$ , the larger the probability of forming the large pores. At smaller  $p_s$ , not only do we obtain smaller pores, but the pores become isolated if we reduce  $p_s$  below a certain value—the percolation threshold  $p_{sc}$  of the pore sites. The size and shape of the pores and related geometrical quantities depend on the percolation mechanism. We will, however, restrict ourselves here to the rigid pores formed by the random distribution of the monodisperse immobile barrier particles.

In the pore space, chains execute their stochastic motion by a “slithering-snake” (reptation [13–15]) algorithm reptating back and forth via both ends (head and tail) selected randomly. An external bias ( $B$ ) is, however, imposed to drive the chains preferentially which is implemented by selecting the hopping probabilities  $\tau_x = (1 + 3B)/4$ ,  $\tau_{-x} = (1 - B)/4$ ,  $\tau_{\pm y} = (1 - B)/4$  along the  $\pm x$  and  $\pm y$  directions. The bias probability  $B$  is introduced to capture the effects of a flow field which may be caused by a pressure gradient. A periodic boundary condition is used to reptate the chains across the boundaries. An attempt to reptate both ends of each chain once is defined as one Monte Carlo step (MCS). This reptation procedure is performed for a sufficiently long time during which we evaluate the mass flux of the polymer chains across the boundaries along the  $x$  direction. For a fixed porosity and polymer concentration  $p$ , the simulation is repeated for a number of independent samples to obtain a reliable estimate of the average flux.

At a nonzero value of the bias  $B$ , there is a net flux of the polymer mass along the direction of the biased field. The rate of change of the flux leads to a mass current ( $i$ ) with the current density  $j = i/L$ . We attempt to analyze the rate of mass transfer of the polymer chains in the frame of linear response description [16], i.e., Darcy’s law,

$$j = L_p \Delta p, \quad (1)$$

where  $\Delta p$  is the pressure difference across the sample, and  $L_p$  is the hydrodynamic permeability. The same relation is also used to study the permeability of the solvent through a membrane in a solution consisting of solvent and solute; in this case  $\Delta p$  corresponds to osmotic pressure resulting from a concentration difference of the solvent. Note that this permeability  $L_p$  is constant only for slow flow in the former and for dilute solution in the later. In complex systems like ours one may question the validity of such linear response theory. However, for simplicity we analyze our data in the framework of an effective linear response. We assume that in the steady state

$$j = \sigma B, \quad (2)$$

where  $B$  is the bias probability and  $\sigma$  is an effective permeability. We should point out that the bias probability is proportional to the pressure difference, and that the

proportionality constant is absorbed in our effective permeability  $\sigma$ . The analysis of  $\sigma$  should exhibit the nonlinear effects of our driven polymer systems, as we will see in the following section.

Thus by calculating the current density at fixed values of the biased field and barrier concentration, we can evaluate the dependence of the permeability on the polymer concentration ( $p$ ) and the size of the chains. With fixed chain length and concentration, we study the dependence of the permeability on barrier concentration and field bias. The biased field and barriers also affect the conformation of the polymer chains and we investigate their effects on the radius of gyration  $R_g$ . The simulations took approximately 1800 h on the Cray-YMP supercomputer.

### III. RESULTS AND DISCUSSION

We use different size lattices to check the finite size effects of our simulations. Most of the production runs were made on a  $100 \times 100$  lattice with 50 independent samples for each polymer concentration  $p$  of monodisperse chains of length  $L_c$  at a fixed porosity  $p_s$ . Figure 1 shows a typical snapshot at a biased field  $B = 0.5$ , porosity  $p_s = 0.9$ , and polymer concentration  $p = 0.4$ . The system has reached the steady state and the chains have already relaxed. Because of the biased field, some stretching of the chains is expected as is seen in this figure. Figure 2 shows a typical plot of the flux mass versus time for various bias probabilities  $B$  at different porosities  $p_s$ . The time taken by the system to reach steady state depends on biased field, porosity, chain length, and concentration. From the slope of the linear plots we evaluate the effective permeability. The permeability versus polymer concentration plot is presented in Fig. 3(a). In a homogeneous system (i.e., porosity  $p_s = 1$ ),

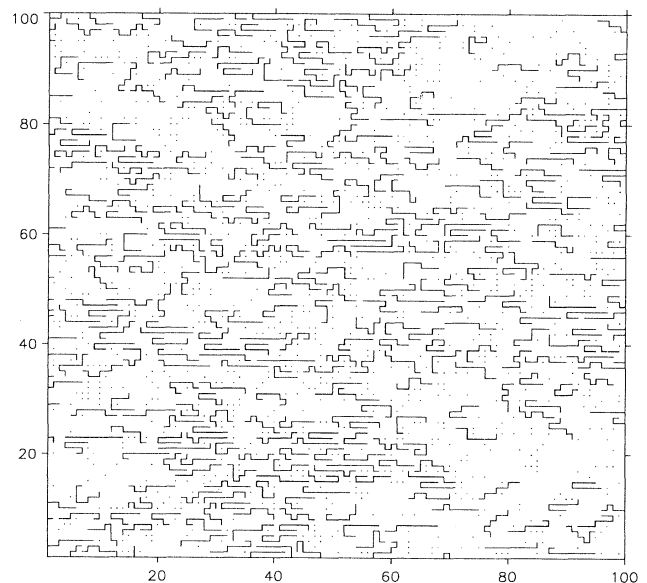


FIG. 1. Snapshot of the system at bias probability  $B = 0.5$  and barrier concentration  $p_b = 0.1$ , with polymer chains of length  $L_c = 10$  and concentration  $p = 0.4$ .

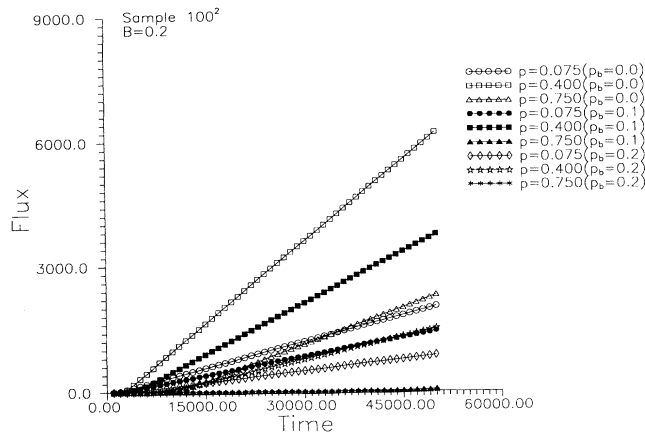


FIG. 2. Flux of mass vs time for various bias  $B = 0.20, 0.50, 0.80$  at porosity  $p_s = 1.00, 0.90, 0.80$  on a  $100 \times 100$  lattice with 50 independent samples. Chains of length  $L_c = 10$  with the polymer concentration  $p = 0.06$  were used.

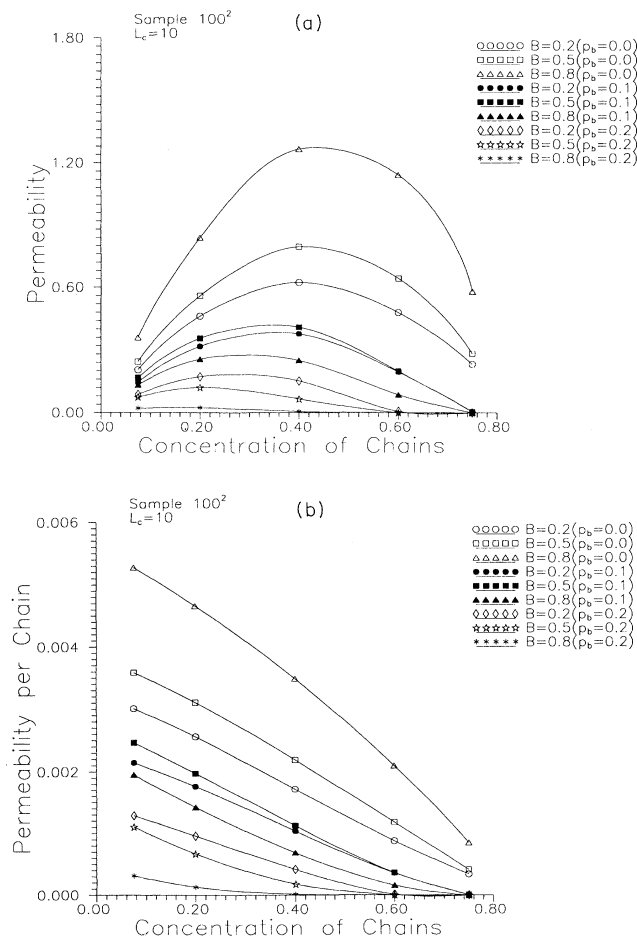


FIG. 3. (a) Permeability  $\sigma$  vs polymer concentration  $p_b$ . (b) Permeability per polymer  $\sigma_p$  versus polymer concentration, for the barrier concentrations  $p_b = 0.0-0.2$  with various values of bias  $B$ . Fifty samples were used with chain length  $L_c = 10$  on a  $100 \times 100$  lattice.

at the bias  $B = 0.2$ , we see that the permeability increases on increasing the polymer concentration until it reaches at a characteristic value  $p_c \approx 0.4$ . At  $p$  above  $p_c$  the permeability decreases on increasing the polymer concentration as the presence of more polymer chains act as mobile barriers. On increasing the bias ( $B = 0.5, 0.8$ ), we observe similar nonmonotonic dependence of the permeability on the polymer concentration  $p$  with a maximum at their characteristic value ( $p_c \approx 0.4$ ). The magnitude of the permeability, however, increases on increasing the bias at  $p_s = 1$  ( $p_b = 0$ ), for the entire range of polymer concentration.

At a lower porosity, we also observe a similar nonmonotonic dependence of the permeability on the polymer concentration. However, reducing the porosity affects the permeability and its behavior significantly as the biased field competes with the barriers at the pore boundaries: (1) The magnitude of the permeability decreases on reducing the porosity. (2) The permeability is no longer a monotonic increasing function of the bias field. It decreases on increasing the bias at  $p_s = 0.9, 0.8$ . We believe that there is a characteristic value of bias,  $B_c$  at each porosity. On increasing the bias, the permeability increases until  $B$  reaches  $B_c$  beyond which it begins to decay at  $p_s < 1$  for a fixed polymer concentration. (3) The characteristic concentration ( $p_c$ ) at which the permeability exhibits a maximum decreases on reducing the porosity.

Let us analyze the data for the permeability per polymer chain,  $\sigma_p = \sigma / N_c$ . Figure 3(b) shows the  $\sigma_p$  versus polymer concentration plot. We note that  $\sigma_p$  decays with the polymer concentration for all values of  $p_b$  and  $B$ . In this figure, we do not have data at very low polymer concentration ( $p$  close to zero), where we expect  $\sigma_p$  to become a constant. The decay of  $\sigma_p$  even at low polymer concentration ( $p \approx 0.1-0.2$ ) in the absence of barriers ( $p_b = 0$ ) is not unexpected, as the chains begin to interfere with each other in the semidilute regime [14]. The critical concentration (a percolation threshold) at which the chains begin to interfere with each other decreases with the chain length [4]. So the chains will begin to interfere at relatively low polymer concentration for longer chains. The decay of  $\sigma_p$  depends strongly on both the bias as well as the porosity. A universal functional dependence is, however, hard to predict from this figure. In the following, we consider polymer chains of fixed length and concentration where these permeabilities  $\sigma_p$  and  $\sigma$  are proportional to each other. Therefore, we consider only the permeability  $\sigma$  of the whole polymer system.

The variation of the permeability with the concentration of the barriers at a polymer concentration  $p = 0.2$  is presented in Fig. 4 for various biased fields. The permeability decreases on reducing (increasing) the porosity (barrier concentration); it decays down to zero near  $p_s = 0.60$ . The nature of the decay of the permeability depends on the bias. At low values of the bias, the permeability decreases almost linearly with  $(1 - p_s)$  in a high porous regime with a relatively slow decay to zero in low porosity regime. At high values of the bias, a rapid decay in the high porous regime is followed by a long tail in the low

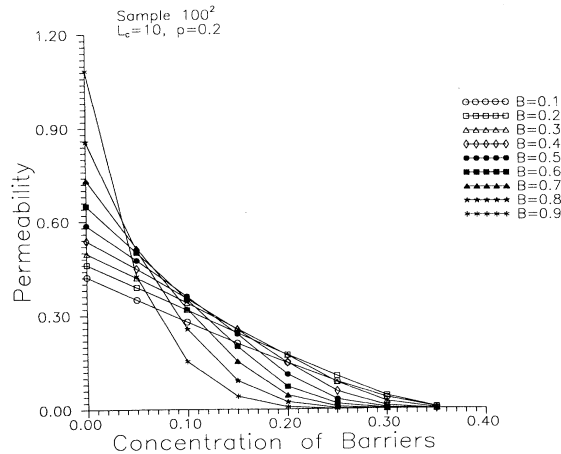


FIG. 4. Permeability  $\sigma$  vs barrier concentration  $p_b$  for chains of length  $L_c = 10$  and concentration  $p = 0.2$ , for the biased field values  $B = 0.1-0.9$ . The lattice size is  $100 \times 100$  with 50 independent samples.

porous regime. These variations suggest that the decay of the permeability with  $(1-p_s)$  cannot be described by a single power law. Furthermore, the value of the bias seems to govern the dependence of permeability on the porosity. With these data, we are not able to establish a universal functional dependence of the permeability  $\sigma(p_s, B)$  on the porosity and the bias  $B$ . However, we hope that our investigations will stimulate further studies that may lead to a more precise prediction of such a functional dependence.

Figure 5 shows the permeability versus bias plot for various values of the barrier concentrations ( $p_b = 0.0-0.35$ ). In absence of barriers ( $p_b = 0.0$ ), the permeability increases on increasing the bias. The rate of increase of permeability depends on the magnitude of the bias: the higher the bias, the larger the rate. Thus the permeability increases nonlinearly on increasing the bias. The presence of barriers, however, leads to a dramatic change in the variation of the permeability. Even at a

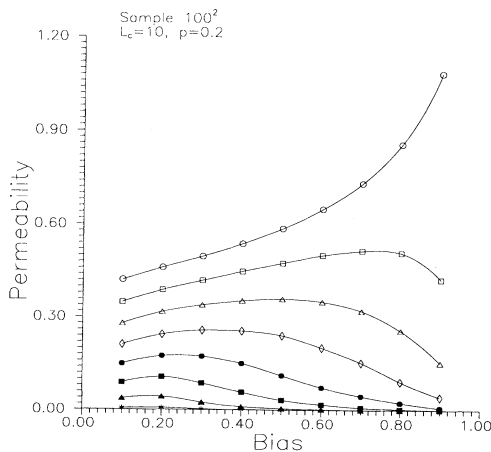


FIG. 5. Permeability  $\sigma$  vs bias  $B$  for barrier concentrations  $p_b = 0.0-0.35$  with the same statistics as in Fig. 4.

small barrier concentration ( $p_b = 0.05$ ), the permeability falls off at higher values of bias ( $p_b \geq 0.7$ , see Fig. 5). The optimum (characteristic) value of bias,  $B_c$ , above which the permeability begins to fall off depends strongly on the barrier concentration. Figure 6 shows the optimum bias versus the barrier concentration plot. The optimum bias seems to decay logarithmically with barrier concentration,  $B_c \sim -\gamma \ln p_b$ , with  $\gamma \approx 0.35$ .

Next, we would like to analyze the dependence of the permeability with the size of the polymer chains. The permeability versus chain length plot is presented in Fig. 7(a) on a log-log scale for various barrier concentrations and biased fields. We see that the permeability decreases on increasing the chain length. A fairly linear fit of the data suggests a power-law dependence of the permeability on the chain length ( $L_c$ ),  $\sigma \sim L_c^{-\alpha}$ , at least in the absence of the impurity barriers. Note that the power-law dependence of the permeability on  $L_c$  remains unchanged at different lattice sizes [see Fig. 7(b)]. The decay exponent  $\alpha$  seems to depend on both the barrier concentration and the biased field; the estimate of  $\alpha$  is presented in Table I. We note that  $\alpha$  increases systematically on increasing  $B$ , which suggests that the exponent is nonuniversal.

For a fixed chain length and concentration ( $L_c = 10$ ,  $p = 0.2$ ), we study the dependence of the radius of gyration on the strength of field bias and barrier concentration. Figure 8 shows the radius of gyration  $R_g$  versus field bias  $B$  for different barrier concentrations. We observe that for barrier concentrations  $p_b \leq 0.15$ , the radius of gyration increases monotonically with increasing field bias  $B$ . The rate of increase is greatest for zero barrier concentration and decreases as the barrier concentration increases. The dependence of the radius of gyration  $R_g$  on barrier concentration  $p_b$  for various biased fields is presented in Fig. 9. For field bias  $B \geq 0.5$ , the radius of gyration decreases monotonically with increasing barrier concentration until about  $p_b = 0.2$ , and fluctuates for  $p_b > 0.2$ . The rate of decay is most rapid for the highest field bias ( $B = 0.9$ ), and decreases as the bias decreases.

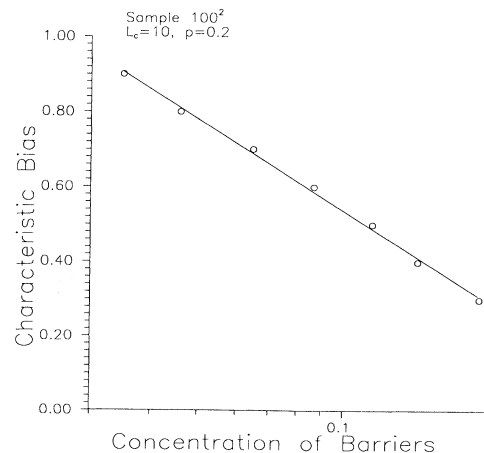


FIG. 6. Characteristic bias  $B_c$  vs barrier concentration  $p_b$  for the polymer concentration  $p = 0.20$  with chain length  $L_c = 10$  on a  $100 \times 100$  lattice with 50 samples.

In Fig. 10 we show on a log-log scale the dependence of the radius of gyration  $R_g$  on the chain length  $L_c$ . At low chain concentration ( $p_c \sim 0.06$ ) and low barrier concentrations ( $p_b \leq 0.2$ ), we observe a power-law dependence of the radius of gyration on the chain length,  $R_g \sim L_c^\nu$ . The power-law exponent  $\nu \sim 0.84-0.94$  does not seem to depend strongly on the bias field (Table I). It shows stronger dependence on the barrier concentration, having a smaller value at a higher barrier concentration.

Finally, we would like to point out the difficulties involved with the linear response description for our polymer system. As we mentioned in Sec. II, Darcy's law (1) is valid as long as the mass-current density is linearly proportional to the pressure difference. If this assertion is valid in our case, then we should obtain a linear fit of the data in a plot of current density  $j$  versus bias  $B$ ; Fig. 11 shows such a plot for various porosities (or barrier concentrations) where a strong deviation from the linear dependence is evident at all porosities. Even in the absence of barriers ( $p_b = 0.0$ ), the current density seems to increase nonlinearly with the bias. On reducing the porosity, the current density shows a nonmonotonic

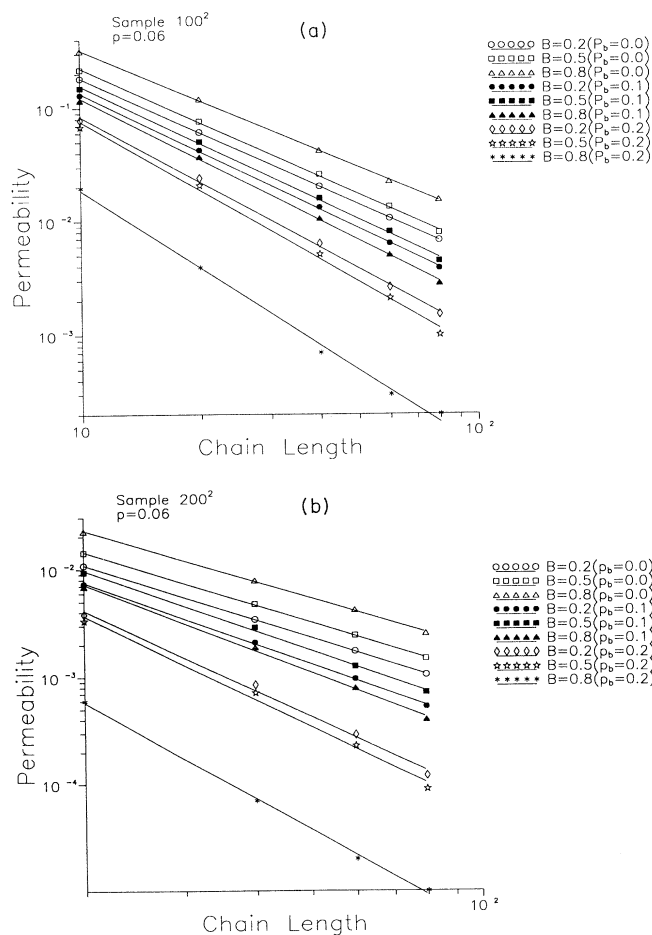


FIG. 7. Permeability  $\sigma$  versus chain length  $L_c$  (log-log plot) for various barrier concentrations and biased fields using (a) a  $200 \times 200$  lattice and (b) a  $100 \times 100$  lattice, with 50 samples at a polymer concentration  $p = 0.06$ .

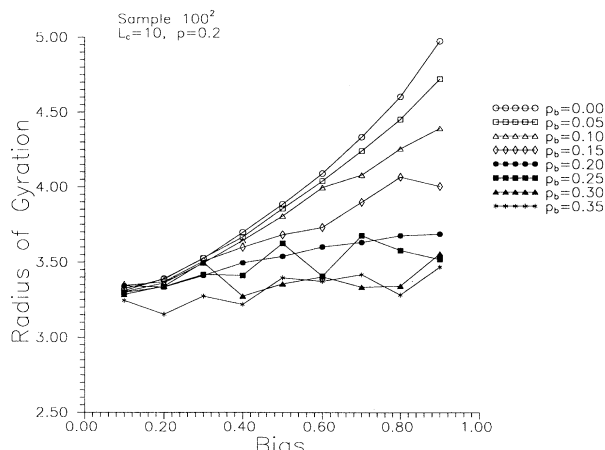


FIG. 8. Radius of gyration  $R_g$  vs bias  $B$  for chains of size  $L_c = 10$ , concentration  $p = 0.2$ , and for barrier concentrations  $p_b = 0.0-0.35$ . The lattice size is  $100 \times 100$  with 50 independent samples.

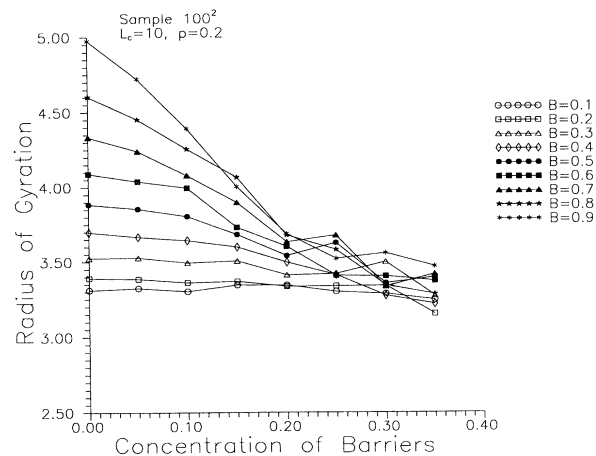


FIG. 9. Radius of gyration  $R_g$  vs barrier concentration  $p_b$  for biased field values  $B = 0.1-0.9$ , with the same statistics as in Fig. 8.

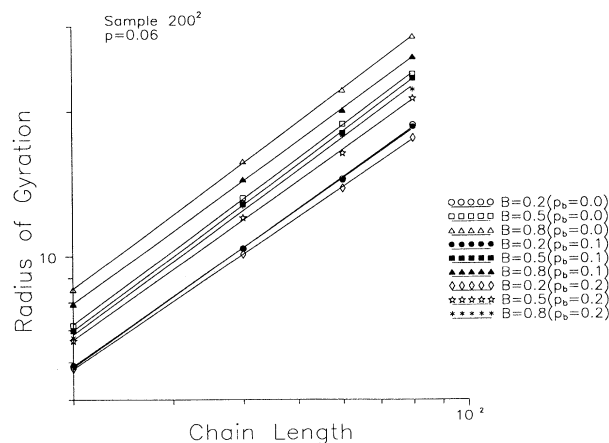


FIG. 10. Radius of gyration  $R_g$  vs chain length  $L_c$  (log-log plot) for various barrier concentrations and biased fields on a  $200 \times 200$  lattice with 50 samples at a polymer concentration  $p = 0.06$ .

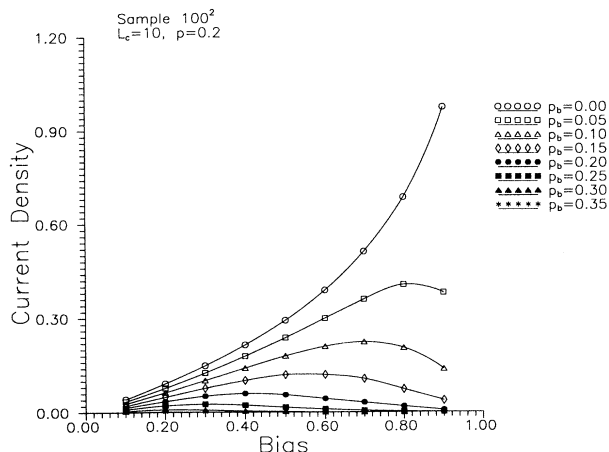


FIG. 11. Current density  $j$  vs bias  $B$  for barrier concentrations  $p_b = 0.0-0.35$ . Chain length  $L_c = 10$ , polymer concentration  $p = 0.2$ , lattice size  $100 \times 100$  with 50 independent samples.

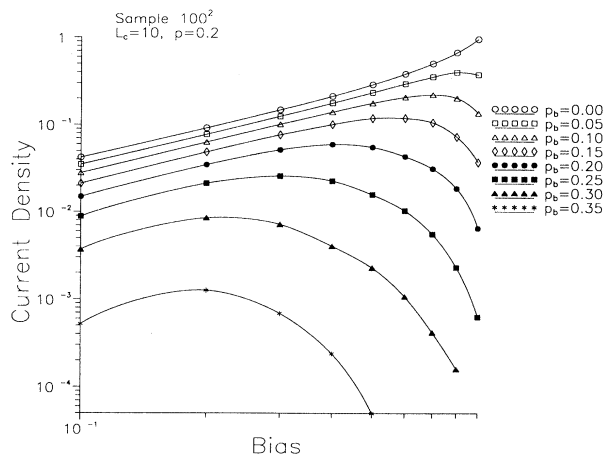


FIG. 12. Current density  $j$  vs bias  $B$  (log-log plot) for barrier concentrations  $p_b = 0.0-0.35$ , with the same statistics as in Fig. 11.

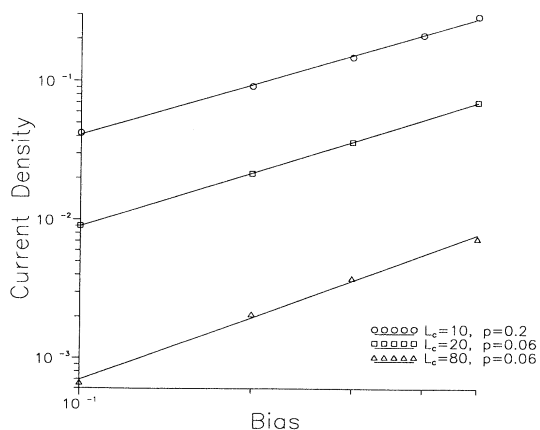


FIG. 13. Current density  $j$  vs bias  $B$  (log-log plot) at zero barrier concentration, for various chain lengths  $L_c$  and concentrations  $p$ :  $L_c = 10$ ,  $p = 0.2$ ,  $L = 100$  (circle);  $L_c = 20$ ,  $p = 0.06$ ,  $L = 200$  (square);  $L_c = 80$ ,  $p = 0.06$ ,  $L = 200$  (triangle), 50 independent samples.

TABLE I. Power-law exponents.

Barrier concentration	bias	$\alpha$	$\nu$
$p_b$	$B$		
0.00	0.20	1.64	0.89
0.00	0.50	1.67	0.91
0.00	0.80	1.77	0.94
0.10	0.20	2.08	0.88
0.10	0.50	2.01	0.93
0.10	0.80	2.29	0.90
0.20	0.20	3.02	0.85
0.20	0.50	3.14	0.86
0.20	0.80	3.73	0.84

dependence on the bias: the current density increases on increasing the bias followed by a decay beyond a characteristic value of the bias ( $B_c$ ). The current density decreases due to competition between the driving bias and the barriers at  $B$  above  $B_c$ . The magnitude of the characteristic bias depends on the barrier concentration,  $B_c$  increases on reducing the barrier concentration. However, at bias below  $B_c$ , linear or nonlinear response description should be applied.

In the low bias regime, we would like to develop a nonlinear approach to understand the nonlinear response of the current density to driving bias. Let us assume that the current density grows with the bias with a power law

$$j = AB^\delta, \quad (3)$$

where  $A$  is a constant and  $\delta$  is a power-law exponent. A plot of the variation of the current density  $j$  with bias  $B$  on a log-log scale is shown in Fig. 12. Although these plots show strong deviations at relatively high values of bias, we do see the linear fits of the data points at low values of the bias particularly at low barrier concentrations ( $p_b = 0.0-0.15$ ); we find  $\delta \approx 1.20$ . So, a power-law response of our driven polymer system does not seem inappropriate although other possibilities cannot be ruled out.

Let us examine the power-law response a little more closely. For simplicity we will not consider barriers ( $p_b = 0.0$ ). Figure 13 shows a plot of current density versus bias on a log-log scale for different chain lengths ( $L_c = 10, 20, 80$ ) at different polymer concentrations. These data were generated at different lattice sizes which should not affect our results since we have not observed severe finite size effects in these simulations. We note that all the data points show an excellent linear fit. However, the slopes of these lines, i.e., the exponent  $\delta$ , seem to depend on the chain length as well as their concentrations,  $\delta \approx 1.20-1.51$  (see Table II).

TABLE II. Nonlinear response exponent.

Chain length	Polymer concentration	$\delta$
$L_c$	$p$	
10	0.20	1.20
20	0.06	1.28
80	0.06	1.51

It is rather difficult to develop a unified approach to such nonlinear response due to the nonuniversal nature of the power-law exponent. Nevertheless, if one chooses a fixed polymer concentration and chain length, such a nonlinear response formula (3) seems reasonable. In any case, this analysis illustrates that the response due to the driving bias in our system is highly nonlinear, and cannot be described by traditional linear response approaches even at low values of the bias.

#### IV. SUMMARY AND CONCLUSION

A computer-simulation model is introduced to study the permeability of the chain polymers through a porous medium. The chains are modeled by the constrained self-avoiding walk while the porous medium is generated from a random distribution of the quenched barriers. An external biased field is applied to drive the chains along the direction of the field. As the chains reptate through the porous medium, there is a net flux along the direction of the field. Using an effective linear response theory, we evaluate the effective permeability. We find several interesting results for the dependence of the permeability on the concentration of the barriers, magnitude of the fields, and the concentration and size of the chains.

The permeability shows a non-monotonic dependence on the polymer concentration. Permeability decays on increasing the barrier concentration ( $p_b$ ). However, the nature of the decay with  $p_b$  depends strongly on the field strength. In the absence of barriers, the permeability increases nonlinearly on increasing the bias. The introduction of quenched barriers strongly affects the dependence of the permeability on the bias due to competition between the bias and the barriers. The permeability decreases on increasing the bias beyond a characteristic value of the bias  $B_c$  which depends on the concentration

of the barriers. The optimum value of the bias ( $B_c$ ) decays logarithmically with barrier concentration,  $B_c \sim -\gamma \ln p_b$ , where  $\gamma \simeq 0.35$ . We find that the permeability depends strongly on the size of the chains. It shows a power-law decay with the chain length,  $\sigma \sim L_c^{-\alpha}$ , with a nonuniversal power-law exponent  $\alpha$  which depends on the barrier concentration ( $\alpha \simeq 1.64-3.73$ , for  $p_b = 0.0-0.2$ ); it is also enhanced on increasing the bias.

For low barrier concentrations ( $p_b \leq 0.15$ ), the radius of gyration increases with increasing field bias, the increase is most rapid when there are no barriers. We observe that for the field bias  $B \geq 0.5$ , the radius of gyration decreases on increasing the barrier concentration, the decrease is most rapid in high field bias. In the dilute limit of chains with low barrier concentrations, the radius of gyration shows a power-law dependence on the chain length,  $R_g \sim L_c^\nu$ , with  $\nu$  depending on the field bias ( $\nu \sim 0.84-0.94$ ).

An alternate approach to study such a nonlinear polymer flow through a porous medium is pointed out. We argue that a power-law response theory could be used as a starting point to capture the nonlinear dependence of the current density on the flow field. We plan to extend this study to systems with more realistic features such as full dynamics of chains, interaction, temperature, etc. We hope that such unusual transport phenomena reported here will stimulate further interest in these areas, both theoretically as well as experimentally.

#### ACKNOWLEDGMENTS

We acknowledge support from the NSF-EPSCoR grant. We thank the Mississippi Center for Supercomputing Research for the computing resources. We thank Rob Lescanec for useful discussion.

- 
- [1] M. Sahimi, *Rev. Mod. Phys.* **65**, 1393 (1993), and references therein; M. Sahimi, *Applications of Percolation* (Taylor and Francis, London, 1994).
- [2] D. Stauffer and A. Aharony, *Introduction to Percolation Theory* (Taylor and Francis, London, 1992).
- [3] T. Duke and J. L. Viovy, *Phys. Rev. E* **49**, 2408 (1994); A. R. Völkel and J. L. Noolandi, *J. Chem. Phys.* **102**, 5506 (1995); G. W. Slater, P. Mayer, S. L. Hubert, and G. Drouin, *Appl. Theor. Electrophoresis* **4**, 71 (1994); M. Muthukumar, *Macromol. Theory Simul.* **3**, 61 (1994).
- [4] J. L. Becklehimer and R. B. Pandey, *J. Stat. Phys.* **75**, 765 (1994).
- [5] A. Cancelliere, C. Chang, E. Foti, D. H. Rothman, and S. Succi, *Phys. Fluids A* **2**, 2085 (1990); D. H. Rothman, *Geophys.* **53**, 509 (1988); *J. Geophys. Res.* **95**, 8663 (1990); C. Baudet, J.-P. Hulin, P. Lallemand, and D. d'Humieres, *Phys. Fluids A* **1**, 507 (1989).
- [6] Y. He and R. B. Pandey, *Phys. Rev. Lett.* **71**, 565 (1993); R. B. Pandey and J. L. Becklehimer, *Phys. Rev. E* **51**, 3341 (1995).
- [7] *Microscopic Simulations of Complex Hydrodynamic Phenomena*, edited by M. Mareschal and B. L. Holian (Plenum, New York, 1992); *Theory, Application and Hardware*, Proceedings of the NATO Advanced Research Workshop on Lattice Gas Methods for PDE's, edited by G. Doolen [*Physica D* **47** (1991)].
- [8] G. A. Kohring, *Physica A* **186**, 97 (1992).
- [9] K. Kehr and K. Binder, in *Application of Monte Carlo Simulation in Statistical Physics*, edited by K. Binder (Springer-Verlag, Berlin, 1986).
- [10] M. A. Knackstedt and X. Zhang, *Phys. Rev. E* **50**, 2134 (1994).
- [11] P. G. de Gennes, *Physica A* **138**, 206 (1986).
- [12] D. A. Hoagland and E. S. Arvanitidou, *Polymer Preprints* **34**, 1059 (1993).
- [13] M. Doi and S. F. Edwards, *The Theory of Polymer Dynamics* (Clarendon, Oxford, 1986).
- [14] P. G. de Gennes, *Scaling Concepts in Polymer Physics* (Cornell University, Ithaca, NY, 1979).
- [15] K. Binder, in *Computational Modeling of Polymers*, edited by J. Bicerano (Marcel Dekker, New York, 1992).
- [16] E. L. Clussler, *Diffusion: Mass Transfer in Fluid Systems* (Cambridge University, Cambridge, 1984).